The site of regulation of light capture in Symbiodinium: Does the peridinin–chlorophyll a–protein detach to regulate light capture?

ARTICLE *in* BIOCHIMICA ET BIOPHYSICA ACTA · APRIL 2014

Impact Factor: 4.66 · DOI: 10.1016/j.bbabio.2014.03.019 · Source: PubMed

Biochimica et Biophysica Acta 1837 (2014) 1227–1234

Contents lists available at ScienceDirect

Biochimica et Biophysica Acta

journal homepage: www.elsevier.com/locate/bbabio

The site of regulation of light capture in *Symbiodinium*: Does the peridinin–chlorophyll *a*–protein detach to regulate light capture?

Atsuko Kanazawa [a,*], Gary J. Blanchard [b], Milán Szabó [c], Peter J. Ralph [c], David M. Kramer [a]

[a] Plant Research Laboratory, R106 Plant Biology Building, Michigan State University, East Lansing, MI 48824-1312, USA
[b] Department of Chemistry, R328, Michigan State University, East Lansing, MI 48824-1322, USA
[c] Plant Functional Biology and Climate Change Cluster (C3), University of Technology, Sydney, PO Box 123 Broadway, NSW 2007, Australia

ARTICLE INFO

Article history:
Received 27 December 2013
Received in revised form 27 March 2014
Accepted 29 March 2014
Available online 8 April 2014

Keywords:
Non-photochemical quenching
Peridinin–chlorophyll *a*–protein
Photoprotection
Photosynthesis

ABSTRACT

Dinoflagellates from the genus *Symbiodinium* form symbiotic associations with cnidarians including corals and anemones. The photosynthetic apparatuses of these dinoflagellates possess a unique photosynthetic antenna system incorporating the peridinin–chlorophyll *a*–protein (PCP). It has been proposed that the appearance of a PCP-specific 77 K fluorescence emission band around 672–675 nm indicates that high light treatment results in PCP dissociation from intrinsic membrane antenna complexes, blocking excitation transfer to the intrinsic membrane-bound antenna complexes, chlorophyll *a*–chlorophyll c_2–peridinin–protein-complex (acpPC) and associated photosystems (Reynolds et al., 2008 *Proc Natl Acad Sci USA* 105:13674–13678).We have tested this model using time-resolved fluorescence decay kinetics in conjunction with global fitting to compare the time-evolution of the PCP spectral bands before and after high light exposure. Our results show that no long-lived PCP fluorescence emission components appear either before or after high light treatment, indicating that the efficiency of excitation transfer from PCP to membrane antenna systems remains efficient and rapid even after exposure to high light. The apparent increased relative emission at around 675 nm was, instead, caused by strong preferential exciton quenching of the membrane antenna complexes associated with acpPC and reaction centers. This strong non-photochemical quenching (NPQ) is consistent with the activation of xanthophyll-associated quenching mechanisms and the generally-observed avoidance in nature of long-lived photoexcited states that can lead to oxidative damage. The acpPC component appears to be the most strongly quenched under high light exposure suggesting that it houses the photoprotective exciton quencher.

1. Introduction

The dinoflagellates, *Symbiodinium* sp. (commonly referred as zooxanthellae) form symbiotic relationships with scleractinian corals, providing photosynthetic products to the coral hosts, in return receiving nitrogen in the form of ammonia and shelter from predators (see [1]). This symbiosis is the foundation upon which coral reefs and their associated diverse ecosystems are built. It is thought that corals expel a small quantity of *Symbiodinium* as part of their regular maintenance under permissive (non-stressed) conditions, e.g. to remove non-functional cells [1–3]. However, certain environmental stresses, such as high temperature and high irradiance, trigger mass expulsion of *Symbiodinium* [4], leading to the bleaching phenomenon that threatens coral reefs worldwide [5]. It has been demonstrated across a wide range of coral species from diverse locations that an increase of only 1–2 °C in mean summertime maximum temperature is sufficient to trigger bleaching [6,7].

Despite intensive study, the underlying basis or triggering mechanism for bleaching has not been identified, though several possibilities have been proposed which impact on various components of the photosynthetic electron transport chain, e.g. impairment of repair mechanisms of the photosystem II (PSII) protein D1 [8,9], the Calvin–Benson-Bassham cycle [10,11], or the production of reactive oxygen species (ROS) [12,13]. There is clear evidence that the conditions of the host–symbiont interaction contribute a large proportion of the sensitivity to bleaching. For example, six out of the nine clades of *Symbiodinium* are currently identified in scleractinian corals (see [14,15]), and they show differential resistance to high temperature bleaching in association with specific host corals [13,16,17].

One of the most striking features of dinoflagellate photosynthesis is the presence of distinctive light harvesting apparatuses. The light harvesting complexes (LHC) of dinoflagellates contain chlorophyll *a* and c_2 and carotenoids, but no chlorophyll *b*. The thylakoid membranes

Abbreviations: acpPC, chlorophyll *a*–chlorophyll c_2–peridinin–protein-complex; Chl, chlorophyll; CW, continuous wave; DDM, n-dodecyl 5-β-d maltoside; LHC, light harvesting complexes; NPQ, non-photochemical quenching; PCP, peridinin–chlorophyll *a*–protein; PSI, photosystem I; PSII, photosystem II; ROS, reactive oxygen species; TB, Tris–borate; TCSPC, time-correlated single photon counting

* Corresponding author. Tel.: +1 517 432 0071.
E-mail addresses: kanazawa@msu.edu (A. Kanazawa), Blanchard@chemistry.msu.edu (G.J. Blanchard), Milan.Szabo@uts.edu.au (M. Szabó), Peter.Ralph@uts.edu.au (P.J. Ralph), kramerd8@msu.edu (D.M. Kramer).

http://dx.doi.org/10.1016/j.bbabio.2014.03.019
0005-2728/

contain intrinsic complexes, called chlorophyll *a*–chlorophyll c_2–peridinin–protein-complex (acpPC), that funnel energy into the reaction centers of photosystem I (PSI) and PSII. In addition, these organisms contain water-soluble LHCs called peridinin–chlorophyll *a*–proteins (PCP), that are peripherally attached to the lumenal side of the thylakoid membrane [18,19]. The carotenoid peridinin allows for the efficient absorption of green light which is transferred with high efficiency to the chlorophyll molecules as it has been modeled recently by ultrafast spectroscopic techniques [20–22] It was also proposed that triplet formation of peridinin molecules prevents PCP from potential photodamage (e.g. [22–24]). There are detailed studies about the excitation energy transfer pathways within PCP and acpPC [25–27], as well as the interplay of the two antenna systems, yet the energy transfer from either PCP or acpPC to the photosystems remains elusive.

The relatively loose binding of PCP to the thylakoid membrane [28] raises the possibility that this complex may dissociate or move between different membrane components to regulate or mediate light absorption, much as state transitions are thought to operate in plants, green alga [29] and cyanobacteria [30]. Indeed, Reynolds et al. [31] found that exposure of *Symbiodinium* cells to photoinhibitory light resulted in a relative increase in the 77 K fluorescence emission band attributable to PCP (at about 675 nm) with respect to that from acpPC (at about 680 nm). This finding was interpreted as reflecting a unique photoprotective mechanism wherein PCP functionally detaches from the acpPC or other intrinsic membrane LHCs. This "detachment model" explains the observed increase in 672–675 nm emission in terms of blocking transfer of excitation energy from PCP to membrane LHCs.

Despite the utilization of this explanation in the field (e.g. [32]), it is important to consider alternative interpretations for the data. Specifically, an increase in 672–675 nm compared to the 686 nm emission could also arise from strong non-photochemical quenching (NPQ) of the longer wavelength band(s), or by a rearrangement of PCP so that it transfers energy into components with smaller emission efficiency at longer wavelengths. We term this possible explanation the "quenching model". The normalization process required to process continuous wave (CW) emission spectra (such as [31,32]) does not allow these alternate explanations to be distinguished.

In this work, we aimed to test these two possibilities using time-resolved fluorescence lifetime measurements. An implicit prediction of the detachment model is that the fluorescence quantum efficiency of PCP would increase upon detachment, resulting in a longer lifetime of its characteristic emission band at 675 nm. In contrast, the quenching model predicts similar rates of transfer of excitation energy from PCP to acpPC regardless of light exposure, and thus similar PCP fluorescence lifetimes, but a more rapid decay of longer wavelength emission components associated with acpPC and reaction centers. Time domain fluorescence lifetime measurements will also allow us to evaluate the possibility that PCP detachment could activate ROS, i.e. the longer the lifetime, the higher the probability that an exciton will be transferred to O_2.

2. Materials and methods

2.1. Symbiodinium strain and culture conditions

Symbiodinium CS-73, clade A, [16] culture was grown in f/2 media ([33], Fritz f/2 algae food A and B, Fritz Industries Inc., Dallas, Texas, USA) at 25 °C with a photoperiod of 14 h at 40 μmol photons m^{-2} s^{-1} photosynthetically active radiation. For the experiments, cultures from late exponential phase (21–24 days old) were used. The isolated *Symbiodinium* cultures in laboratory condition have the doubling time of 2 to 20 days depending on the species (e.g. [34], see also [35–38]). In our growth condition, the cells around 3 weeks old are routinely used for the experiments (see [16]; see also Results and discussion in this paper for chlorophyll fluorescence, NPQ and diatoxanthin data). The cells were harvested at 9 A.M. to avoid diurnal physiological changes.

2.2. Isolation of PCP and acpPC

Symbiodinium cultures were harvested by centrifugation at 8000 *g* for 10 min at 4 °C. The pellet was re-suspended in 4–5 mL of ice-cold TB buffer (100 mM Tris–borate pH 8.0, 2 mM $MgCl_2$, 2 mM Na_2EDTA, 1 mM phenylmethyl–sulphonyl fluoride), and cells were ruptured by three passes through a French pressure cell at ~8×10^7 Pa. The resulting lysate was centrifuged at 500 *g* for 10 min at 4 °C to remove unbroken cells and cell debris. The crude homogenate was incubated with 50% $(NH_4)_2SO_4$ at 4 °C for 10 min, and centrifuged for 10 min at 8,000 *g* at 4 °C. The orange-colored supernatant containing the water-soluble PCP (sPCP) [39] was stored on ice in complete darkness for further use. The pellet was washed in 1 mL of ice-cold TB buffer and centrifuged at 21,000 *g* for 20 min at 4 °C. The pellet, containing the thylakoid membranes, was re-suspended in ice-cold TB buffer at a chlorophyll (Chl) $a + c$ content of 250 μg mL^{-1}, and the sample was incubated with n-dodecyl 5-β-d maltoside (DDM) (Sigma-Aldrich Inc.) at a detergent:Chl *a* ratio of 60:1 (*v*/*v*). The membranes were solubilized in darkness using gentle stirring at 4 °C for 20 min, and the resulting suspension was centrifuged for 20 min at 21,000 *g*. The soluble supernatant was loaded with a Chl $a + c$ content of 120 μg mL^{-1} onto a continuous sucrose density gradient obtained by freezing and thawing 25% sucrose in TB buffer containing also 0.03% DDM. The gradients were centrifuged for 16 h at 150,000 *g* at 4 °C using a swing-out rotor (TH-641, Thermo Scientific Inc.) with an ultracentrifuge (Sorvall WX-80, Thermo Scientific Inc.). The dark-brown colored band containing the acpPC [40] was removed with a syringe from the sucrose gradient and stored on ice in complete darkness for further use. For spectroscopic measurements, the samples were diluted to a chlorophyll content of ~2 μg mL^{-1}.

2.3. Determination of chlorophyll content

The Chl $a + c$ content of the samples, extracted by 90% acetone, was determined spectrophotometrically using a spectrophotometer (Cary-Varian UV–VIS) according to Jeffrey and Humphrey [41].

2.4. High light treatments

Whole cell cultures were exposed to white LED light of 1000 μmol m^{-2} s^{-1} for 4 h at room temperature, and were immediately frozen in EPR tubes (Norell Inc.) under liquid nitrogen.

2.5. CW fluorescence emission spectra

To obtain 77 K fluorescence emission spectra, samples were frozen in quartz EPR tubes (3 mm diameter) and immersed in liquid nitrogen. Excitation from 440 or 520 nm diode lasers and fluorescence emission measured by a spectrometer (Ocean Optics HR200 + ER) were coupled by a bifurcated quartz optical fiber.

2.6. Time-resolved fluorescence emission experiments (TCSPC)

All fluorescence lifetime data were acquired using a time-correlated single photon counting (TCPSC) instrument that has been described in detail elsewhere [42]. Briefly, the light source is a CW passively mode-locked, diode-pumped Nd:YVO_4 laser (Spectra Physics Vanguard) that produces 2.5 W average power at 355 nm and 532 nm, at 80 MHz repetition rate with 13 ps pulses. The 355 nm output of the Nd:YVO_4 laser pumps a cavity-dumped dye laser (Coherent 702-2), which operates at 446 nm (Stilbene 420 dye, Exciton) or 520 nm (Coumarin 500 dye, Exciton), producing 5 ps pulses. The repetition rate of the dye laser is 4 MHz, controlled by cavity dumping electronics (Gooch &

Housego, Inc.). For both excitation wavelengths, the laser output is linearly polarized with a polarization extinction ratio of *ca.* 100. The pulse train from the dye laser is divided, with one portion directed to a reference photodiode (Becker & Hickl PHD-400-N), and the other portion directed to the sample. Emission is collected using a 40× reflecting microscope objective (Ealing). The collected emission is separated into polarization components parallel (0°) and perpendicular (90°) to the vertically polarized excitation pulse using a polarizing cube beam splitter (Newport, extinction ratio ≥500:1). The parallel and perpendicular polarized signal components are detected simultaneously using microchannel plate photomultiplier tubes (MCP-PMT, Hamamatsu R3809U-50), each equipped with a subtractive double monochromator (Spectral Products CM-112). The detection electronics (Becker & Hickl SPC-132) resolve the parallel and perpendicular transients separately, yielding *ca.* 40 ps response functions for each detection channel. The G factor was evaluated by exciting the sample with horizontally polarized light and collecting both horizontal and vertical polarization components of the emission. The right angle collection geometry of the experiment renders both emission polarization components identical under this excitation condition, and the difference in the intensity of the two emission components is a direct measure of the G factor. Data acquisition, detector bias, and collection wavelength are all controlled using an in-house written LabVIEW® (National Instruments) program on a PC. Fluorescence lifetime decays are calculated from the polarized transients according to $I_{fl}(t) = I_{||}(t) + 2I_{\perp}(t)$. To account for minor variations in the TCSPC fluorescence emission amplitudes, which are caused by variations in frozen sample properties, the intensity at each wavelength integrated over the complete kinetic trace was normalized to match the continuous wave emission intensity at the respective emission wavelength. Global fits were performed to both CW and time resolved emission data using the global fitting routine in Origin (OriginLab).

2.7. Pulse amplitude modulated (PAM) chlorophyll fluorometry

Symbiodinium sample suspensions were dark-adapted for 10 min ('Dark' samples) and after exposure to 1000 μmol photons m^{-2} s^{-1} for 4 h ('Light' samples, see Section 2.4.). The maximum quantum yield (F_V / F_M, where $F_V = F_M - F_0$) was measured by using a Water-PAM Fluorometer (Walz GmbH, Effeltrich, Germany) on *Symbiodinium* cells that were dark-adapted for 10 min ('Dark' samples). Weak measuring light (~0.15 μmol photons m^{-2} s^{-1}, gain: 2–4) was used to determine minimum fluorescence (F_0) and a saturating pulse (0.8 s, >3500 μmol photons m^{-2} s^{-1}) was used to determine the dark-adapted maximum fluorescence (F_M). The effective quantum yield after illumination (F_q / F_M', where $F_q = F_M' - F_0'$) was recorded on 'Light' samples with the same parameters as for F_V / F_M parameters; however, background illumination was provided by the LEDs of Water-PAM with the same PFD as for the light treatment (see Section 2.4.) The F_0' and F_M' parameters reflect the minimal and maximal fluorescence in the light-adapted state. Non-photochemical quenching (NPQ) was calculated by using the Stern–Volmer data treatment; $NPQ = F_M / F_M' - 1$.

2.8. High performance liquid chromatography (HPLC)

The photoprotective (diadinoxanthin, diatoxanthin and β-carotene) pigment concentrations of the algal symbionts were determined using reverse-phase HPLC (with slight modification from [32]). At each sampling time point (see Section 2.4.) 5 mL cultures were taken from 'Dark' and 'Light' samples (see above), vacuum-filtered onto GF/F filter paper (Whatman) with a diameter of 25 mm, snap frozen in liquid nitrogen and placed in a freezer at −80 °C until further analysis. Subsequently, the filter papers containing the samples were transferred to 5 mL of HPLC-grade 100% acetone and the pigments were extracted using an ultrasonic probe (Sonic and Material Inc. USA; Model-VC50T; 50 W, 20 KHz) for 30 s. Samples were kept in the dark and on ice during sonication. The acetone solution containing the extracted samples were vortexed for 30 s, kept in the dark at −20 °C for 12 h, vortexed again for 30 s and 3 mL of the homogenate was passed through a 0.2 μm PTFE 13 mm syringe filter (Micro-Analytix Pty Ltd) and placed into an amber HPLC glass vial. The vials were loaded into the autosampler and maintained at 4 °C and in darkness. For HPLC analyses, the pigment absorbance spectrum was measured from 270 to 700 nm using a photodiode array detector with a 4.3 nm bandwidth (Waters, Australia). Calibration and quality assurance were performed by using external calibration standards of each pigment (DHI, Hørsholm, Denmark). Empower Pro 2 software quantified chlorophyll *a* concentrations at 665 nm, and all other pigments at 450 nm through peak integration. The de-epoxidation ratio (a measure of diadinoxanthin conversion to the photoprotective diatoxanthin) was calculated as the diatoxanthin pool divided by the total diatoxanthin + diadinoxanthin pool (Dt / [Dt + Dd]).

3. Results and discussion

3.1. Fluorescence emission spectra of CS-73 at 77 K

Fig. 1 shows the fluorescence emission spectra (black squares) of control and high light treated samples with excitation at 520 and 440 nm. After high light treatment, a pronounced shoulder appeared at 675 nm relative to 686 nm when excited with green (520 nm) light that is preferentially absorbed by PCP. In contrast, relatively small differences in emission were observed when samples were excited with blue (440 nm) light that is absorbed preferentially by the chlorophylls, consistent with previous work [31,32]. Table 1 shows chlorophyll fluorescence parameters taken from whole cells at room temperature just prior to freezing for the 77 K fluorescence emission spectra, showing that the light treatment induced strong increases in NPQ, decreases in maximal quantum efficiency (decreased Fq / F_M' compared to F_V / F_M) and strong increases in the de-epoxidation ratio.

The six 77 K fluorescence emission spectra (isolated PCP, acpPC, the whole cells treated with growth light excited with 440 nm and 520 nm, and the whole cells treated with high light excited with 440 nm and 520 nm) were fit globally to sets of Gaussian components. The remaining data were fit using non-linear least square routine, as described in the Materials and methods, allowing both the center wavelength and the bandwidth to vary. The goodness of fit, as estimated by R^2 values, increased rapidly as the number of Gaussian components was increased from one to up to seven. For the sake of parsimony, we constrained our fitting procedure to the number of components that resulted in R^2 values greater than 0.996. This threshold was reached at 5 Gaussian components, and larger numbers of components resulted in only minimal improvement. The results of the fits are shown in Fig. 1 A–D. The dashed curves in the figure represent the shapes of the individual components and the solid curves represent the predicted emission spectra at the wavelengths used for kinetics assays (see below), based on the sum of contributions from the five fit components. The center wavelengths and bandwidths of components 1 and 2 from the 5-component fit were consistent with PCP and acpPC, respectively, as measured from Gaussian fits to emission spectra of isolated PCP (Component 1) and acpPC (Component 2) taken at 77 K with excitation at 520 and 440 nm respectively. Measured in our hands, the 77 K CW fluorescence emission spectra (Fig. 2A) and lifetimes (Fig. 2B) for isolated PCP and acpPC were about 3 and 5 ns, consistent with previous work [31,32]. Components 3, 4 and 5 were consistent with emission from longer wavelength antenna associated with Photosystem II (Component 3) and combination of Photosystem I and fluorophores in the vicinity (Components 4 and 5) [21,22].

The relative contributions from the five Gaussian components were dependent on excitation wavelength and exposure to high light (Table 2). When excited with green wavelengths, the relative emission by PCP (component 1) relative to that from component 3 (at 686 nm)

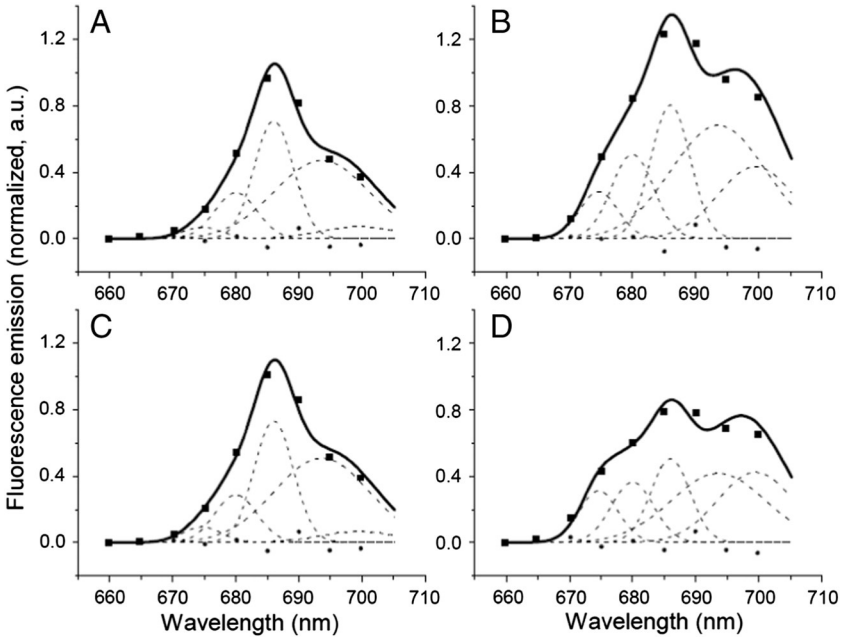

Fig. 1. Fluorescence emission spectra and global Gaussian fits for control and high light treated cells of *Symbiodinium* CS-73 cells at 77 K. Control samples (Panels A and C) were taken from low (40 μmol photons m^{-2} s^{-1}) growth light conditions while high light treated samples (Panels B and D) were exposed to 1000 μmol photons m^{-2} s^{-1} for 4 h as described in Materials and methods. Frozen samples were excited with 440 nm (Panels A and B) or at 520 nm (Panels C and D). The filled symbols represent the fluorescence emission values, normalized to that at 685 nm, taken at the wavelengths used for TCSPC experiments. The solid lines represent the best global fits to the data using five Gaussian components, as described in the text. The dashed lines represent the individual Gaussian curves.

increased about 5-fold after high light exposure. This trend was also seen in blue-excited samples, though the relative emission from PCP was smaller, with only a 3.5-fold increase, consistent with the high ratio of green-absorbing peridinin relative to blue absorbing chlorophyll in PCP. Overall, these results are consistent with either an increase in emission from PCP or a decrease in emission from longer-wavelength components, as reported by [31].

3.2. Fluorescence lifetime decay kinetics

To distinguish between the quenching and detachment models, we conducted spectrally resolved time-correlated single photon counting (TCSPC) experiments on control and high light treated cells, as well as isolated PCP and acpPC (Fig. 2). Fig. 3 A–D shows the fluorescence emission decay kinetics for intact, control and high light treated cells at wavelengths from 660 nm to 695 nm upon excitation by 5 ps, 446 nm and 520 nm laser pulses. The amplitudes of fluorescence kinetics were normalized to the peak of 675 nm emission in each sample because the fluorescence lifetimes (and thus most likely the fluorescence yield values) at this wavelength were nearly completely independent of environmental conditions (see below). The kinetics observed at different wavelengths were distinct, reflecting differences in the initial absorption and progression of exciton transfer between complexes. The rise kinetics reflect both the time resolution of the TCSPC instrument and the excitation of individual components. Compared to the control samples, the high light treated samples exhibited smaller integrated fluorescence signals (normalized to that at 675 nm), while the decay kinetics of longer wavelength emission components were substantially faster. Importantly, high light treatment did not induce noticeable long-lived fluorescence components at shorter wavelengths, similar to isolated PCP, as would be expected if excitation transfer from PCP were inhibited by detachment.

These general behaviors are seen more clearly in the spectra for fluorescence emission constructed from TCSPC traces shown for selected times after laser excitation of control and light treated samples excited at 446 and 520 nm (Fig. 4). Shorter wavelength (higher energy) components on the blue edge of the emission spectrum tended to rise and decay more rapidly, resulting in peaks that appeared at earlier times. Excitation at 446 nm, which predominantly excites chlorophylls in acpPC, produced transient emission with a peak at 680 nm that appeared with a halftime of about 50–100 ps. In contrast, excitation at 520 nm produced an additional, transient, peak at 675 nm, with very rapid (~10 ps) rise and decay (~150–200 ps) time, consistent with preferential excitation of PCP. In both cases, the emission spectra shifted to longer wavelengths at longer delay times, reflecting the sequential transfer of excitation from shorter to longer wavelength antenna and reaction center components.

The fluorescence emission spectra at each time point for the data shown in Fig. 4 were fit to the five Gaussian components described above (Fig. 5 A–H). The close correspondence between the curves and measured data points indicated that the five-component model accounted reasonably well for the observed phenomena. Based on our global fits, we estimated the kinetics of formation and decay for each component as shown for each treatment (Fig. 5 A–H). Components 4 and 5 were summed in the data presented in Fig. 5 because they behaved kinetically similarly, because our data only extends to 710 nm preventing us from sufficiently resolving their individual conditions.

Excitation of control cells at 520 nm resulted in rapid (within earliest 10 ps time point) rise in PCP fluorescence, which decayed with a lifetime of approximately 150–200 ps. (It is important to note that the fluorescence decay, especially following high light treatment, was sufficiently rapid that it overlapped with the instrumentation rise time, so that rates of decay were likely underestimated by the apparent lifetimes, but our conclusions do not depend on precise deconvolution of these effects). The decay of PCP fluorescence coincided with a rise

Table 1
Chlorophyll fluorescence parameters and relative diatoxanthin (Dt) content (de-epoxidation ratio) of dark-adapted and pre-illuminated (4 h, 1000 μmol photons m^{-2} s^{-1} white light, at 26 °C) *Symbiodinium* CS-73 cells. Chlorophyll fluorescence parameters are shown as mean (S.E.) ($n = 4$).

	F_V / F_M or F_q / F_M'	NPQ ($F_M / F_M' - 1$)	De-epoxidation ratio (Dt / [Dd + Dt])
Dark	0.618 (0.009)	0	0.005 (0.002)
Light	0.111 (0.005)	1.8 (0.19)	0.348 (0.013)

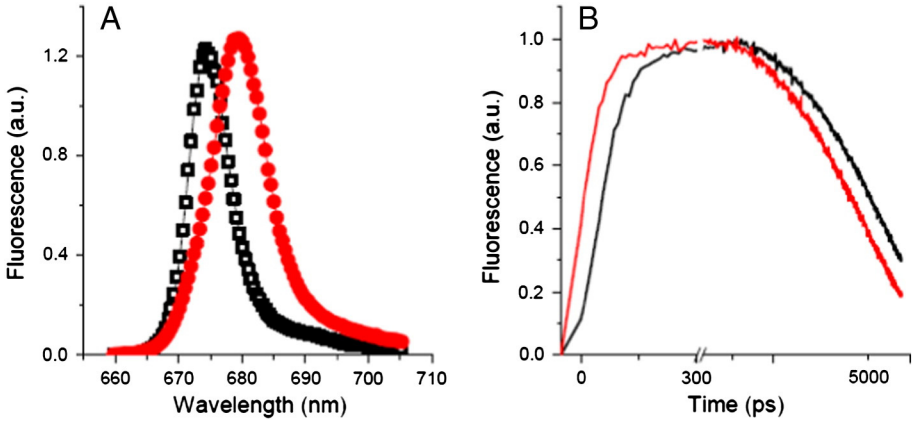

Fig. 2. Fluorescence emission spectra and decay kinetics for PCP and acpPC at 77 K. Samples were isolated and treated as described in Materials and methods in the main body of the text. Panel A shows the emission spectra of isolated PCP (black open square) and acpPC (red closed circle) with excitation at 520 nm and 440 nm respectively. Panel B shows fluorescence lifetime decay kinetics of isolated PCP (black line) and acpPC (red line). Note split time base at 300 ps, with log scale after the break. Samples were excited at 520 nm for PCP, and 446 nm for acpPC.

in acpPC emission and longer wavelength acpPC and components 3 (Fig. 5), suggesting transfer of excitation energy from PCP to acpPC and PSII on the order of 150 ps, consistent with unpublished results cited in [43]. We observed relatively weak PCP emission when samples were excited at 446 compared to 520 nm, consistent with the expected excitation spectra of PCP and acpPC. The smaller PCP-attributable emission appeared with a (slower) rise time of about 60 ps, possibly indicating unresolved contributions from acpPC in the deconvolution, or excitation migration from acpPC to PCP.

Components 4 and 5 appeared with a risetime of about 200–300 ps, but were largely independent of excitation wavelength, suggesting that transfer of excitation energy occurred from acpPC or other integral membrane antenna, rather than directly from PCP. In control cells, fluorescence from acpPC, PSII and the sum of components 4 and 5 decayed with lifetimes of approximately 1.1, 1.8 and 2.5 ns, respectively. These lifetimes were somewhat more rapid than found for isolated acpPC at 77 K [25–27], implying the presence of effective exciton quenching, either photochemical or NPQ-related, even in control cells. A similar phenomenon, more efficient quenching in the intact system than the isolated antenna, has also been observed in plants (e.g. [44,45]).

The rise and decay kinetics of the PCP-associated fluorescence did not change appreciably after high light exposure, indicating that the excitonic coupling between PCP and membrane-associated antenna complexes was largely unaffected by light treatment. In contrast, the lifetimes for acpPC, PSII and the sum of components 4 and 5 decreased after high light treatment by a factor of about 2–3, to 0.4, 0.5 and 0.95 ns. These results indicate the appearance of efficient exciton quenchers associated with these antenna complexes after light treatment, leading to increased non-radiative decay of excitation energy from the longer wavelength components after high light treatment.

3.3. Where is the site of high-light photoprotection?

The detachment model has several attractive features, nicely explaining the increase in 675 nm fluorescence relative to that from other components in the context of the unusual properties of PCP. This model also had the distinct advantage of being a readily testable hypothesis, clearly predicting an increase in PCP fluorescence yield and lifetime after detachment from thylakoid LHC components upon light treatment. In this work, we tested the detachment model directly in *Symbiodinium* clade A before and after exposure of cells to high light. Contrary to predictions of the detachment model, we found that PCP fluorescence lifetime remained rapid even after exposure to high light (Figs. 4 and 5) indicating that the transfer of light energy from PCP to intrinsic membrane light harvesting complexes remains efficient.

Instead, we observed strong, preferential quenching of longer wavelength components. These results are consistent with the appearance of an efficient exciton quencher in the membrane LHCs, but not with excitonic detachment of PCP, which should result in longer lifetime for emission around 675 nm, as seen in the kinetics of isolated (and thus detached) PCP. Fluorescence from acpPC was the most affected by high light, suggesting that it, or closely associated complexes, is a primary site of quenching, possibly by lumen pH-activated diadinoxanthin/diatoxanthin associated NPQ [46–49], though a mechanism for dinoflagellate NPQ is unresolved [24,27,50]. Overall, the simplest model is that the major quencher occurs in acpPC, though we cannot exclude the appearance of quenchers in the core PSI and PSII components. It is also noteworthy that all 5 Gaussian components, and not just those attributed to acpPC and PSII, show evidence of NPQ, implying that either the separate quenchers are activated in PSII and PSI antenna complexes, or that excitation energy can migrate between PSI, PSII and acpPC and can thus be quenched by a single pool of quenchers.

Table 2
Relative amplitude of fluorescence emission components (Gaussian). Data are averages (standard deviations) of three separate samples, each measured in triplicate. CT = control and HL = high light treatment. The signals were normalized so that the sums of amplitudes for all components for each treatment were unity.

	Component 1	Component 2	Component 3	Component 4	Component 5
	PCP	acpPC			
Peak (nm)	674.7	680.0	686.0	693.6	699.5
Width (nm)	6.1	6.7	6.2	15	12
Amplitude CT ex440 nm	0.029 (0.001)	0.127 (0.001)	0.301 (0.003)	0.483 (0.005)	0.060 (0.008)
Amplitude CT ex520 nm	0.037 (0.002)	0.125 (0.002)	0.294 (0.003)	0.493 (0.012)	0.051 (0.012)
Amplitude HL ex440nm	0.068 (0.007)	0.133 (0.003)	0.195 (0.003)	0.400 (0.001)	0.204 (0.066)
Amplitude HL ex520 nm	0.102 (0.009)	0.129 (0.003)	0.167 (0.004)	0.332 (0.010)	0.270 (0.007)

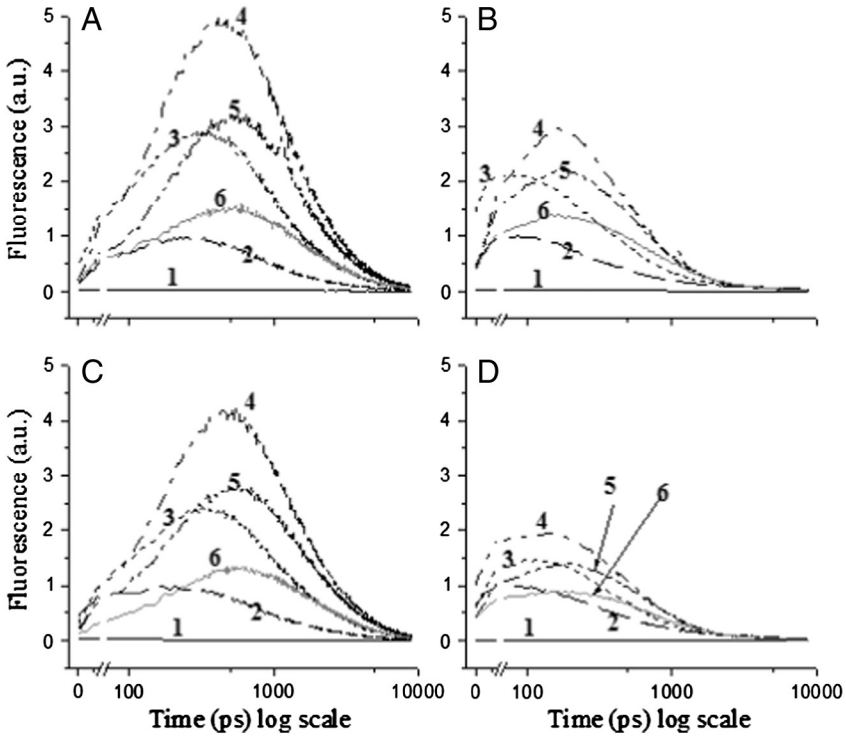

Fig. 3. Representative fluorescence lifetime decay kinetics at 77 K in log scale. The excitation wavelength was 446 nm for A (control) and B (high light-treated), and 520 nm for C (control) and D (high light-treated). The fluorescence emission spectra were taken at 660 nm (1: solid line. The decay of this spectrum was very fast so that the amplitude looks almost negligible.), 675 nm (2: dash line), 680 nm (3: dot line), 685 nm (4: dash dot line), 690 nm (5: dash dot dot line) and 695 nm (6: gray solid line) respectively.

Based on comparisons of decay kinetics upon excitation with 446 and 520 nm light, we observed no evidence for changes in PCP excitation transfer to PSI-associated antenna (components 4 and 5, Fig. 5 D and H). This result argues against large contributions from PCP state transitions to regulation of light capture, at least under our conditions. However, it does not rule out the possibility of direct PCP to PSI excitation transfer, as long as it is not strongly affected by high light.

Overall, we conclude that the exciton transfer connection between PCP and acpPC is efficient and robust even after high light treatment. Instead, the previously observed shift in continuous wave emission appears related to activation of NPQ in membrane-associated antenna, likely in acpPC. It is still possible that PCP detachment can occur under some conditions not tested in our experiments. However, long-lived excitons produced by detached PCP would likely potentiate (through

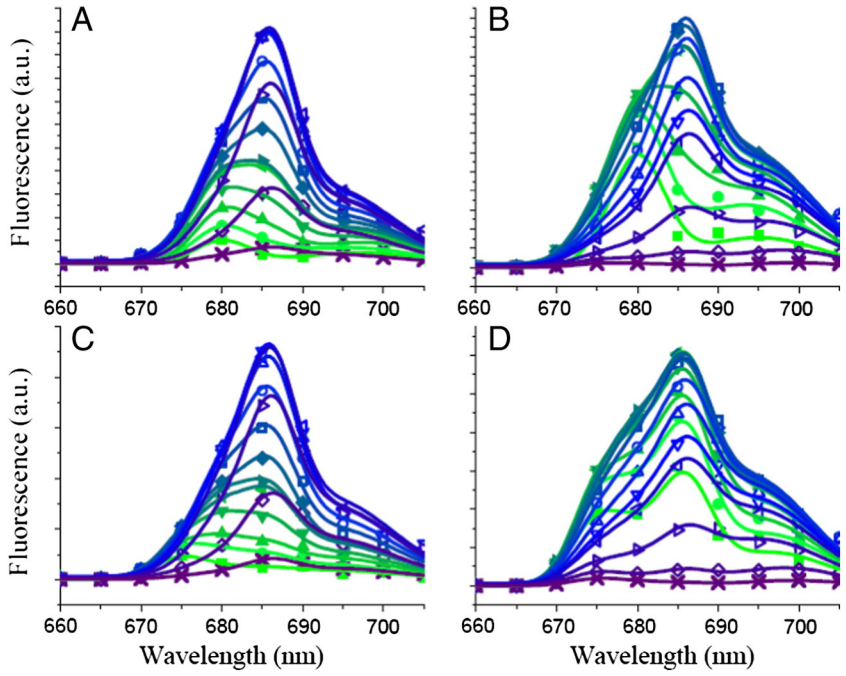

Fig. 4. Time-resolved fluorescence emission spectra of *Symbiodinium* CS-73 whole cells at 77 K. Samples were treated as in Fig. 1, with control samples shown in Panels A and C. Excitation was at 446 nm (Panels A and B) or 520 nm (Panels C and D). Data at selected times following excitation are shown, 0 (■), 29 (●), 49 (▲), 78 (▼), 107 (◀), 117 (▶), 147 (◆), 176 (□), 244 (○), 342 (△), 450 (▽), 537 (◁), 948 (▷), 2072 (◇), and 4876 (✖) ps, respectively. The curves represent best fits to simulated curves using the global fit procedure described in the text.

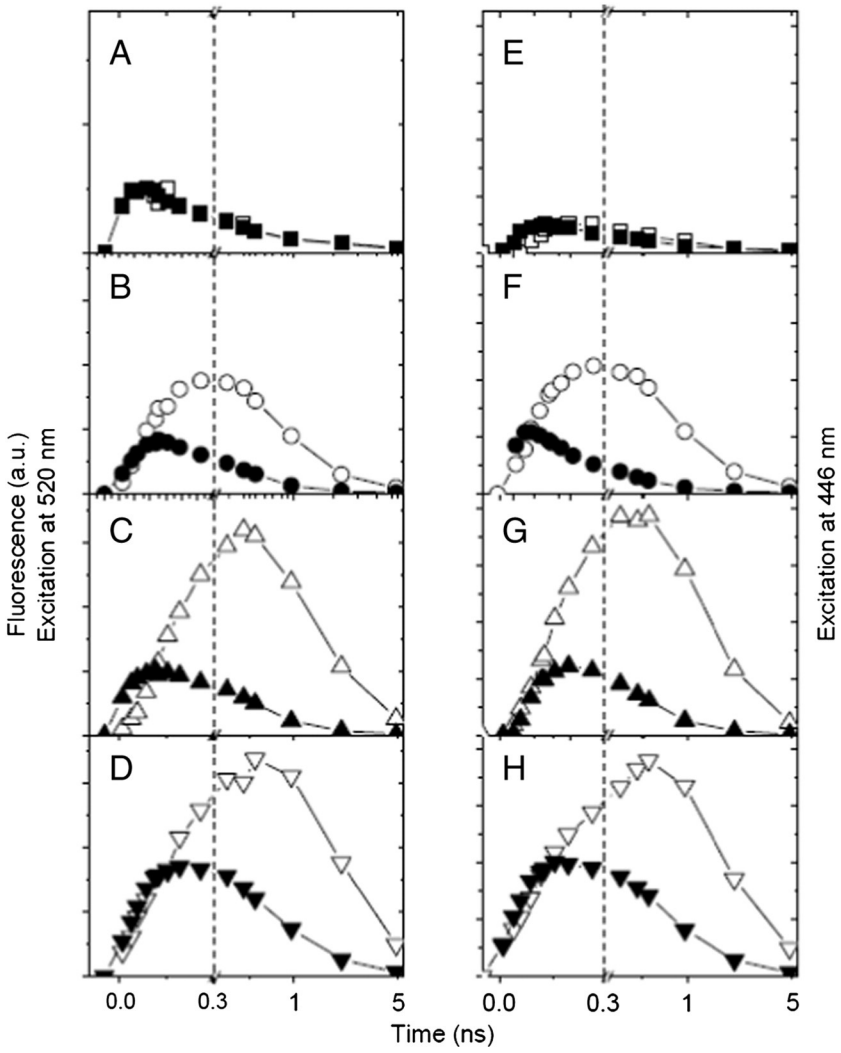

Fig. 5. The kinetics of formation and decay for fluorescence spectral components for *Symbiodinium* CS-73 whole cells at 77 K. Data from control and high light treated samples are indicated by the open and closed symbols. Panels A–D were obtained with excitation at 520 nm, and Panels E–H with excitation at 446 nm. Kinetics represent PCP (Panels A, E), acpPC (Panels B, F), component 3 (Panels C and G, attributed to PSII and associated antenna), and the sum of components 4 and 5 (Panels, D and H, attributed to PSI and associated antenna). For clarity, the *Y*-axis scales for Panels A and E were multiplied by 2. Note split time base at 300 ps, with log scale after the break, as indicated by the dashed vertical line.

interaction with O_2) rather than prevent photodamage, and it is generally observed that natural photosynthesis regulates the antenna to minimize exciton lifetime to avoid generation of reactive oxygen species (e.g. [51,52]). We thus expect strong selection pressure for maintaining strong coupling of PCP to membrane antenna complexes and its regulatory components.

Acknowledgments

The authors thank Professor Anthony Larkum for insightful discussions. This research was funded by Chemical Sciences, Geosciences, and Biosciences, Office of Basic Energy Sciences, Office of Science, US Department of Energy (award number DE-FG02-91ER20021 to D.M.K., supporting work at MSU) and the Australian Research Council (award number DP-110105200 to P.J.R., supporting work at UTS).

References

[1] S.K. Davy, D. Allemand, V.M. Weis, Cell biology of cnidarian–dinoflagellate symbiosis, Microbiol. Mol. Biol. Rev. 76 (2012) 229–261.
[2] R.J. Jones, D. Yellowlees, Regulation and control of intracellular algae (=zooxanthellae) in hard corals, Philos. Trans. R. Soc. Lond. Ser. B Biol. Sci. 352 (1997) 457–468.
[3] W.K. Fitt, Cellular growth of host and symbiont in a cnidarian–zooxanthellar symbiosis, Biol. Bull. 198 (2000) 110–120.
[4] P.J. Ralph, R. Gademann, A.W.D. Larkum, Zooxanthellae expelled from bleached corals at 33 degrees C are photosynthetically competent, Mar. Ecol. Prog. Ser. 220 (2001) 163–168.
[5] O. Hoegh-Guldberg, Climate change, coral bleaching and the future of the world's coral reefs, Mar. Freshwat. Res. 50 (1999) 839–866.
[6] Y. Loya, K. Sakai, K. Yamazato, H. Nakano, H. Sambali, R. van Woesik, Coral bleaching: the winners and the losers, Ecol. Lett. 4 (2001) 122–131.
[7] A.A. Venn, J.E. Loram, H.G. Trapido-Rosenthal, D.A. Joyce, A.E. Douglas, Importance of time and place: patterns in abundance of *Symbiodinium* clades A and B in the tropical sea anemone *Condylactis gigantea*, Biol. Bull. 215 (2008) 243–252.
[8] S. Takahashi, S. Whitney, S. Itoh, T. Maruyama, M. Badger, Heat stress causes inhibition of the de novo synthesis of antenna proteins and photobleaching in cultured *Symbiodinium*, Proc. Natl. Acad. Sci. U. S. A. 105 (2008) 4203–4208.
[9] R. Hill, C.M. Brown, K. DeZeeuw, D.A. Campbell, P.J. Ralph, Increased rate of D1 repair in coral symbionts during bleaching is insufficient to counter accelerated photoinactivation, Limnol. Oceanogr. 56 (2011) 139–146.
[10] R.M. Lilley, P.J. Ralph, A.W.D. Larkum, The determination of activity of the enzyme Rubisco in cell extracts of the dinoflagellate alga *Symbiodinium* sp. by manganese chemiluminescence and its response to short-term thermal stress of the alga, Plant Cell Environ. 33 (2010) 995–1004.
[11] R.J. Jones, O. Hoegh-Guldberg, A.W.D. Larkum, U. Schreiber, Temperature-induced bleaching of corals begins with impairment of the CO_2 fixation mechanism in zooxanthellae, Plant Cell Environ. 21 (1998) 1219–1230.
[12] M.P. Lesser, Oxidative stress causes coral bleaching during exposure to elevated temperatures, Coral Reefs 16 (1997) 187–192.
[13] D. Tchernov, M.Y. Gorbunov, C. de Vargas, S.N. Yadav, A.J. Milligan, M. Häggblom, P.G. Falkowski, Membrane lipids of symbiotic algae are diagnostic of sensitivity to thermal bleaching in corals, Proc. Natl. Acad. Sci. U. S. A. 101 (2004) 13531–13535.
[14] M.A. Coffroth, S.R. Santos, Genetic diversity of symbiotic dinoflagellates in the genus *Symbiodinium*, Protist 156 (2005) 19–34.

[15] X. Pochon, R.D. Gates, A new Symbiodinium clade (Dinophyceae) from soritid foraminifera in Hawai'i, Mol. Phylogenet. Evol. 56 (2010) 492–497.
[16] L. Buxton, S. Takahashi, R. Hill, P.J. Ralph, Variability in the primary site of photosynthetic damage in *Symbiodinium* sp. (dinophyceae) exposed to thermal stress, J. Phycol. 48 (2012) 117–126.
[17] P.L. Fisher, M.K. Malme, S. Dove, The effect of temperature stress on coral–*Symbiodinium* associations containing distinct symbiont types, Coral Reefs 31 (2012) 473–485.
[18] B.J. Norris, D.J. Miller, Nucleotide sequence of a cDNA clone encoding the precursor of the peridinin–chlorophyll a–binding protein from the dinoflagellate *Symbiodinium* sp, Plant Mol. Biol. 24 (1994) 673–677.
[19] E. Hofmann, P.M. Wrench, F.P. Sharples, R.G. Hiller, W. Welte, Structural basis of light harvesting by carotenoids: peridinin–chlorophyll–protein from *Amphidinium carterae*, Science 272 (1996) 1788–1791.
[20] F.J. Kleima, M. Wendling, E. Hofmann, E.J.G. Peterman, R. van Grondelle, H. van Amerongen, Peridinin chlorophyll a protein: relating structure and steady-state spectroscopy, Biochemistry 39 (2000) 5184–5195.
[21] T. Polívka, R.G. Hiller, H.A. Frank, Spectroscopy of the peridinin–chlorophyll-a protein: insight into light-harvesting strategy of marine algae, Arch. Biochem. Biophys. 458 (2007) 111–120.
[22] D.M. Niedzwiedzki, J. Jiang, C.S. Lo, R.E. Blankenship, Low-temperature spectroscopic properties of the peridinin–chlorophyll a–protein (PCP) complex from the coral symbiotic dinoflagellate *Symbiodinium*, J. Phys. Chem. B 117 (2013) 11091–11099.
[23] M.T.A. Alexandre, D.C. Lührs, I.H.M. van Stokkum, R. Hiller, M.-L. Groot, J.T.M. Kennis, R. van Grondelle, Triplet state dynamics in peridinin–chlorophyll-a–protein: a new pathway of photoprotection in LHCs? Biophys. J. 93 (2007) 2118–2128.
[24] M. Di Valentin, E. Salvadori, G. Agostini, F. Biasibetti, S. Ceola, R. Hiller, G.M. Giacometti, D. Carbonera, Triplet–triplet energy transfer in the major intrinsic light-harvesting complex of *Amphidinium carterae* as revealed by ODMR and EPR spectroscopies, Biochim. Biophys. Acta 1797 (2010) 1759–1767.
[25] D. Zigmantas, R.G. Hiller, V. Sundstrom, T. Polívka, Carotenoid to chlorophyll energy transfer in the peridinin–chlorophyll-a–protein complex involves an intramolecular charge transfer state, Proc. Natl. Acad. Sci. U. S. A. 99 (2002) 16760–16765.
[26] T. Polívka, I.H.M. van Stokkum, D. Zigmantas, R. van Grondelle, V. Sundström, R.G. Hiller, Energy transfer in the major intrinsic light-harvesting complex from *Amphidinium carterae*, Biochemistry 45 (2006) 8516–8526.
[27] D.M. Niedzwiedzki, J. Jiang, C.S. Lo, R.E. Blankenship, Spectroscopic properties of the chlorophyll a–chlorophyll c2–peridinin–protein-complex (acpPC) from the coral symbiotic dinoflagellate *Symbiodinium*, Photosynth. Res. 120 (2014) 125–139.
[28] N. Nassoury, L. Fritz, D. Morse, Circadian changes in ribulose-1,5-bisphosphate carboxylase/oxygenase distribution inside individual chloroplasts can account for the rhythm in dinoflagellate carbon fixation, Plant Cell 13 (2001) 923–934.
[29] A.V. Ruban, M.P. Johnson, Dynamics of higher plant photosystem cross-section associated with state transitions, Photosynth. Res. 99 (2009) 173–183.
[30] S. Joshua, C.W. Mullineaux, Phycobilisome diffusion is required for light-state transitions in cyanobacteria, Plant Physiol. 135 (2004) 2112–2119.
[31] J.M. Reynolds, B.U. Bruns, W.K. Fitt, G.W. Schmidt, Enhanced photoprotection pathways in symbiotic dinoflagellates of shallow-water corals and other cnidarians, Proc. Natl. Acad. Sci. U. S. A. 105 (2008) 13674–13678.
[32] R. Hill, A.W.D. Larkum, O. Prášil, D.M. Kramer, M. Szabó, V. Kumar, P.J. Ralph, Light-induced dissociation of antenna complexes in the symbionts of scleractinian corals correlates with sensitivity to coral bleaching, Coral Reefs 31 (2012) 963–975.
[33] R.R.L. Guillard, Culture of phytoplankton for feeding marine invertebrates, in: W.L. Smith, M.H. Chanley (Eds.), Culture of Marine Invertebrate Animals, Springer US, New York, 1975, pp. 29–60.
[34] F.P. Wilkerson, D. Kobayashi, L. Muscatine, Mitotic index and size of symbiotic algae in Caribbean Reef corals, Coral Reefs 7 (1988) 29–36.
[35] E.M. Deane, R.W. O'Brien, Isolation and axenic culture of *Gymnodinium microadriaticum* from *Tridacna maxima*, Br. Phycol. J. 13 (1978) 189–195.
[36] W.K. Fitt, R.K. Trench, The relation of diel patterns of cell division to diel patterns of motility in the symbiotic dinoflagellate *Symbiodinium microadriaticum* Freudenthal in culture, New Phytol. 94 (1983) 421–432.
[37] S.S. Chang, B.B. Prézelin, R.K. Trench, Mechanisms of photoadaptation in three strains of the symbiotic dinoflagellate *Symbiodinium microadriaticum*, Mar. Biol. 76 (1983) 219–229.
[38] S.L. Domotor, C.F. D'Elia, Nutrient uptake kinetics and growth of zooxanthellae maintained in laboratory culture, Mar. Biol. 80 (1984) 93–101.
[39] R. Iglesias-Prieto, N.S. Govind, R.K. Trench, Apoprotein composition and spectroscopic characterization of the water-soluble peridinin–chlorophyll a–proteins from three symbiotic dinoflagellates, Proc. R. Soc. B 246 (1991) 275–283.
[40] R. Iglesias-Prieto, N.S. Govind, R.K. Trench, Isolation and characterization of three membrane-bound chlorophyll–protein complexes from four dinoflagellate species, Philos. Trans. R. Soc. Lond. Ser. B Biol. Sci. 340 (1993) 381–392.
[41] S. Jeffrey, G. Humphrey, New spectrophotometric equations for determining chlorophyll a, b, c1 and c2 in higher plants and natural phytoplankton, Biochem. Physiol. Pflanz. 165 (1975) 191–194.
[42] H.A. Pillman, G.J. Blanchard, Effects of ethanol on the organization of phosphocholine lipid bilayers, J. Phys. Chem. B 114 (2010) 3840–3846.
[43] F.J. Kleima, E. Hofmann, B. Gobets, I.H.M. van Stokkum, R. van Grondelle, K. Diederichs, H. van Amerongen, Förster excitation energy transfer in peridinin–chlorophyll-a–protein, Biophys. J. 78 (2000) 344–353.
[44] A.J. Young, D. Phillip, A.V. Ruban, P. Horton, H.A. Frank, The xanthophyll cycle and carotenoid-mediated dissipation of excess excitation energy in photosynthesis, Pure Appl. Chem. 69 (1997) 2125–2130.
[45] A.V. Ruban, D. Phillip, A.J. Young, P. Horton, Excited-state energy level does not determine the differential effect of Violaxanthin and Zeaxanthin on chlorophyll fluorescence quenching in the isolated Light-Harvesting Complex of Photosystem II, Photochem. Photobiol. 68 (1998) 829–834.
[46] H.A. Frank, A. Cua, V. Chynwat, A. Young, D. Gosztola, M.R. Wasielewski, The lifetimes and energies of the first excited singlet states of diadinoxanthin and diatoxanthin: the role of these molecules in excess energy dissipation in algae, Biochim. Biophys. Acta 1277 (1996) 243–252.
[47] O. Hoegh-Guldberg, R.J. Jones, Photoinhibition and photoprotection in symbiotic dinoflagellates from reef-building corals, Mar. Ecol. Prog. Ser. 183 (1999) 73–86.
[48] J.D. Robison, M.E. Warner, Differential impacts of photoacclimation and thermal stress on the photobiology of four different phylotypes of *Symbiodinium* (PYRRHOPHYTA), J. Phycol. 42 (2006) 568–579.
[49] K.E. Ulstrup, R. Hill, M.J.H. van Oppen, A.W.D. Larkum, P.J. Ralph, Seasonal variation in the photo-physiology of homogeneous and heterogeneous *Symbiodinium* consortia in two scleractinian corals, Mar. Ecol. Prog. Ser. 361 (2008) 139–150.
[50] V. Šlouf, M. Fuciman, S. Johanning, E. Hofmann, H.A. Frank, T. Polívka, Low-temperature time-resolved spectroscopic study of the major light-harvesting complex of *Amphidinium carterae*, Photosynth. Res. 117 (2013) 257–265.
[51] E. Tyystjärvi, N. King, M. Hakala, E.-M. Aro, Artificial quenchers of chlorophyll fluorescence do not protect against photoinhibition, J. Photochem. Photobiol. B Biol. 48 (1999) 142–147.
[52] S. Santabarbara, I. Cazzalini, A. Rivadossi, F.M. Garlaschi, G. Zucchelli, R.C. Jennings, Photoinhibition *in vivo* and *in vitro* involves weakly coupled chlorophyll–protein complexes, Photochem. Photobiol. 75 (2002) 613–618.